www.sciencetranslationalmedicine.org/cgi/content/full/2/28/28ra29/DC1

Supplementary Materials for

Brief Suppression of *Abcc8* Prevents Autodestruction of Spinal Cord After Trauma

J. Marc Simard,* S. Kyoon Woo, Michael D. Norenberg, Cigdem Tosun, Zheng Chen, Svetlana Ivanova, Orest Tsymbalyuk, Joseph Bryan, Douglas Landsman, Volodymyr Gerzanich

*To whom correspondence should be addressed. E-mail: msimard@smail.umaryland.edu

Published 21 April 2010, *Sci. Transl. Med.* **2**, 28ra29 (2010)
DOI: 10.1126/scitranslmed.3000522

This PDF file includes:

Methods
Table S1. Clinical cases.
Fig. S1. Custom antibody is specific for SUR1.
Fig. S2. Rat model of cervical hemicord contusion used to incite progressive hemorrhagic necrosis with minimal primary white matter damage.
Fig. S3. Cervical hemicord contusion incites progressive hemorrhagic necrosis with minimal primary white matter damage.
References
Movie S1. Rats 1 week after SCI treated with *Abcc8*-Scr versus *Abcc8*-AS.

SUPPLEMENTAL MATERIALS

SUPPLEMENTAL METHODS

Human spinal cords

The Miami Project to Cure Paralysis provided spinal cords from 7 cases of SCI (Table S1) and from 3 control cases (2 males; ages 28–44 years; cause of death: pneumonia, ischemic heart disease, respiratory failure). Five of the SCI cases studied here were also studied previously (*1*). In accordance with Fleming et al. (*1*) and references therein, spinal cord injuries were classified on the basis of their histological appearance as

Table S1: Clinical cases

Case number	Time of survival	Age	Gender	Spinal level epicenter	Spinal level remote	Nature of accident	Type of injury
119	2 days	37	m	C3	T4	altercation	M
162	3 days	84	m	C4	T10	fall	M
175	5 days	33	m	T2	T10	MVA	C
176	5 days	88	m	C4	T10	MVA	C
206	5 days	16	m	T8	T3	MVA	C
222	3 days	33	m	C6	T9	MVA	C
238	3 days	59	m	C3	T10	MVA	M

Abbreviations: MVA, motor vehicle accident; M, massive compression type injury, C, contusion type injury.

‘contusion’, or ‘massive compression’. Contusion injuries were characterized by an intact pia and relative preservation of the anatomical relations of various elements of the spinal cord, and variable degrees of injury ranging from involvement of the entire cross-sectional area to large usually asymmetric areas of tissue damage. Massive compression injuries were characterized by disruption of the pia and severe distortion and disruption of spinal cord parenchyma.

Spinal cords were removed within 24 h of death and were fixed in neutral buffered formalin for several weeks. In all cases, tissue samples from the epicenter of the SCI, from the penumbra near the epicenter, and from remote portions of the spinal cord above or below the injury were obtained (Table S1).

Immunolabeling

Blocks of spinal cord tissues were dehydrated, embedded in paraffin, cut into sets of 6 μm thick sections and placed on positively charged glass slides. One set of sections was stained with hematoxylin and eosin (H&E), and the remaining sets were used for immunohistochemistry. Paraffin sections were de-paraffinized by heating to 70° C for 15 min, followed by three 5-min washes in xylene. For antigen retrieval, sections were placed in 10% target retrieval solution (DAKO S1699) and incubated in a pressure cooker for 20 min at 121° C. For immunolabeling, sections were permeabilized (0.2% Triton X-100 for 10 min), blocked (5% goat serum for 1 h), then incubated with the custom anti-SUR1 antibody with high specificity (fig. S1A and B) described below (1:500; 1 h at RT then 48 h at 4° C). Omission of primary antibody was used as a control (fig. S1C and D). Neurons and endothelium were co-labeled using NeuN (1:100;

48 h; Chemicon, MAB372) and von Willebrand factor (1:100; 48 h; Chemicon, MAB3442).

For each SCI patient, expression of SUR1 in tissues from the penumbra adjacent to the epicenter was compared to expression in remote tissues using quantitative immunohistochemistry, as previously described in this laboratory (*2*). All sections were immunolabeled as a single batch. Montages of cord sections from each patient were acquired using uniform parameters of magnification and exposure. For each section, regions of interest (ROI) were first defined separately for grey matter and white matter within one ventral quadrant of the cord. For penumbral sections, we utilized the ventral quadrant with the greatest signal intensity. For remote sections, we utilized the ventral quadrant with the least signal intensity, which closely approximated the signal intensity in the spinal cords of control patients without SCI. Specific labeling for SUR1 was defined as pixels with signal intensity >2.5 times that of background. The area occupied by pixels with specific labeling was used to determine the percent area with specific labeling (% ROI).

Custom antibody to SUR1

A part of the rat SUR1 cDNA (Protein Id, NP_037171; amino acid 598–965) was subcloned into pQE31 (Qiagen) to overexpress the protein in a hexa-histidine-tagged form in bacterial cells. The fusion protein was purified with a Ni^{+}-agarose column and used to raise antibodies in rabbits by a commercial service (Covance).

Total lysates were prepared from COS7 cells transfected with an empty vector or an expression vector encoding FLAG-tagged hamster SUR1 (gift from Dr. Shyng,

Oregon Health and Science University) using a lysis buffer [50 mM Tris-HCl (pH 7.8), 150 mM NaCl, 1% Triton X-100, 1 mM EDTA, and protease inhibitor cocktail (Roche)]. 40 μg of the lysates were separated on a 3–8% acrylamide gel and blotted onto a PVDF membrane. To detect the FLAG-SUR1, the membrane was incubated with anti-FLAG antibody M2 or anti-SUR1 antibody in PBS containing 0.1% Tween 20 and 5% nonfat milk. The blots were then incubated with a secondary antibody conjugated with horseradish peroxidase and the bands were detected by enhanced chemiluminescence (Pierce).

Total lysates from COS7 cells transfected with a control empty vector (fig. S1A lane 1, S1B lane 1) or with an expression vector encoding FLAG-tagged SUR1 (fig. S1A lanes 2 and 3, S1B lanes 2 and 3) were examined by immunoblot using FLAG monoclonal M2 antibody (fig. S1A) or the custom anti-SUR1 polyclonal antibody (fig. S1B). Both antibodies detected the same band at ~140 kDa, as well as higher molecular weight products believed to be due to poly-ubiquitination of SUR1 (*3*). Note that neither antibody detected any specific band from lysates from cells transfected with a control vector (fig. S1A lane 1, S1B lane 1), consistent with a high specificity of the antibody.

The custom antibody was used for immunolabeling of human tissues, utilizing the protocol detailed above. Specificity of labeling was confirmed by demonstrating that, in adjacent tissue sections: (i) the same cellular structures were labeled by the anti-SUR1 antibody and by *in situ* hybridization for *ABCC8* mRNA (fig. 2E); (ii) omission of primary antibody yielded no labeling (fig. S1C versus D).

Spinal cord injury in rat

A rat model of unilateral cervical SCI, which has been characterized in detail (*4, 5*) and used by us previously (*6, 7*), was implemented here with minor modifications. Without treatment in this model, there is minimal primary injury to white matter, but extensive progressive hemorrhagic necrosis that produces bilateral secondary injury to ascending and descending white matter tracts innervating the thoracic, lumbar and sacral gray matter controlling truncal stability, lower extremity function and bladder function.

Female Long-Evans rats (~11 weeks; 225-250 gm; Harlan) were anesthetized (Ketamine, 60 mg per kg plus Xylazine, 7.5 mg per kg, i.p.) and the head was mounted in a stereotaxic apparatus (Stoelting). Using aseptic technique and intra-operative magnification (Zeiss operating microscope with co-axial lighting), the spine was exposed dorsally from C3 to T3 via a 3-cm midline incision and subpereosteal dissection of the paraspinous muscles. The ear bars were removed and the animal was repositioned so that it was supported from the spinous process of T2 (Spinal Adaptor, Stoelting) and the snout. On the left side, the entire lamina of C7 and the dorsal half of the pedicle of C7 were removed using a 1.9-mm diamond burr (#HP801-019, DiamondBurs.Net) and a high-speed drill, with care taken to avoid mechanical and thermal injury to the underlying dura and spinal cord (fig. S2). The dura was exposed by sharply removing the interlaminar ligaments rostral and caudal to the lamina of C7 and any remaining ligamentum flavum. The guide tube containing the impactor (*4*) was angled 5° medially and was positioned using the manipulator arm of the stereotaxic apparatus. The impactor (1.55-mm tip diameter, 57 mm length, 1.01 gm) was carefully positioned on the dura near the left C8 nerve root, with the caudal edge of the impactor

in line with the caudal edge of the C8 nerve root at the axilla, and the medial edge of the impactor 0.3 mm medial to the dorsolateral sulcus. The impactor was activated by releasing a 10 gm weight from a height of 25 mm inside the guide tube. The impact caused an immediate, forceful flexion of the trunk and of the ipsilateral lower extremity. Within 2 min, a 2-mm bruise involving the dorsolateral cord and extending up to the dorsolateral sulcus was apparent through the translucent dura. Animals that did not experience a strong flexor reaction, or whose bruise appeared less prominent than usual were excluded from further study.

The rostro-caudal positioning of the impactor was chosen so that the contralateral cord would be driven into the caudal portion of the contralateral C7 pedicle (*contrecoup*). The medio-lateral positioning was chosen to avoid full impact to the dorsal horn, which tends to produce extensive bilateral primary hemorrhage. Within 2 min of injury, a hemorrhagic contusion was evident through the intact dura that involved the lateral surface of the cord extending up to the sulcus, but not more medially. Examining coronal sections of the cord at the epicenter 30 min after injury showed that the primary hemorrhage was limited to the ipsilateral cord, including the dorsolateral funiculus and dorsal horn, with some extension into the ventral horn (fig. S3). However, 24 h later (in untreated animals), secondary hemorrhage typically extended through much of the ipsilateral cord and well into the contralateral gray and white matter (fig. S3) (*6, 7*).

After injury, the surgical site was flushed with 1 ml of NS, the musculature replaced over the spine and the skin incision stapled. Rats were nursed on a heating pad to maintain rectal temperature ~37° and were given 10 ml of glucose-free normal saline subcutaneously. Food and water were placed within easy reach to ensure that

they were able to eat and drink without assistance. Bladder function was assessed by observing for urination and if needed, manual emptying was carried out using the Credé maneuver.

SUPPLEMENTAL RESULTS

Video 1. Rats 1 week after SCI treated with *Abcc8*-Scr versus *Abcc8*-AS

This video is available upon request and may be obtained by contacting the corresponding author directly.

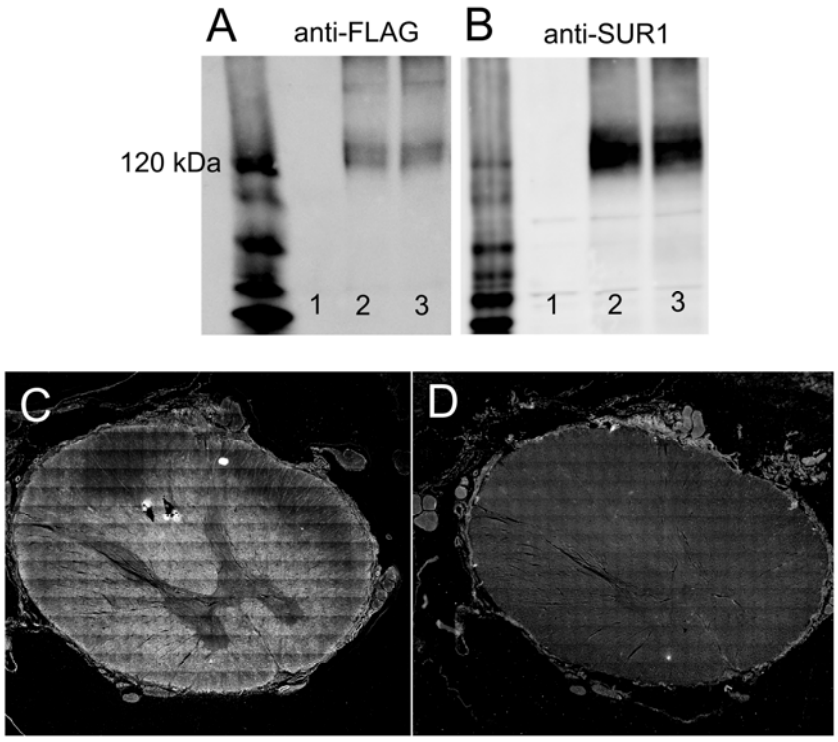

Fig. S1. Custom antibody is specific for SUR1. (**A** and **B**) Immunoblots of cell lysates visualized using anti-FLAG antibody (**A**) then stripped and visualized using custom anti-SUR1 antibody (**B**); the lysates were from COS7 cells transfected with empty vector (Lane 1) or with vector containing FLAG-tagged-SUR1 plasmid (Lanes 2,3); the ladder (first lane in each blot) confirms the appropriate molecular mass of ~140 kDa for SUR1. (**C,D**) Adjacent sections of injured human spinal cord (patient 206) immunolabeled for SUR1 using the custom antibody described and visualized using a CY3-conjugated anti-rabbit secondary antibody (**C**), or omitting the primary antibody and using the secondary antibody alone as a negative control (**D**); the montages shown were constructed from multiple individual images, and positive labeling is shown in white pseudocolor.

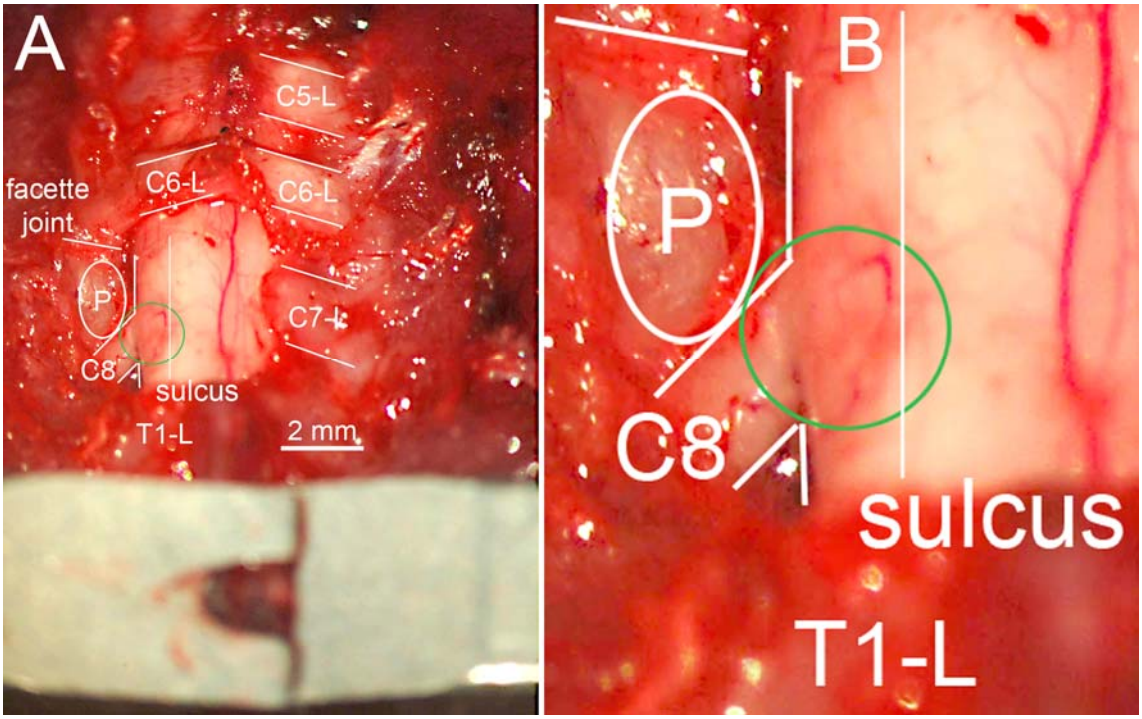

Fig. S2. Rat model of cervical hemicord contusion used to incite progressive hemorrhagic necrosis with minimal primary white matter damage. (**A,B**) Low (**A**) and high (**B**) magnification photomicrographs of the surgical exposure used for cervical hemi-cord contusion injury; after removing the spinous processes of C5 to T1, the left lamina of C7 and the interlaminar ligaments and ligamentum flavum at C7, the left hemicord at C7 is visualized through the translucent dura; the anatomical details visualized include the laminae (L) of cervical (C) and thoracic (T) vertebral levels C5 through T1, the left facette joint between C6 and C7, the C8 nerve root exiting the spinal canal caudal to the left pedicle (P) of C7, and the dorsolateral sulcus of the spinal cord, from which emerges the rootlets of the dorsal roots; note the metallic clamp on the spinous process of T2 in (**A**); the 1.55 mm diameter impactor used to produce contusion injury is directed at an angle of 5° medially and is positioned to strike the spinal cord in the area denoted by the green circle.

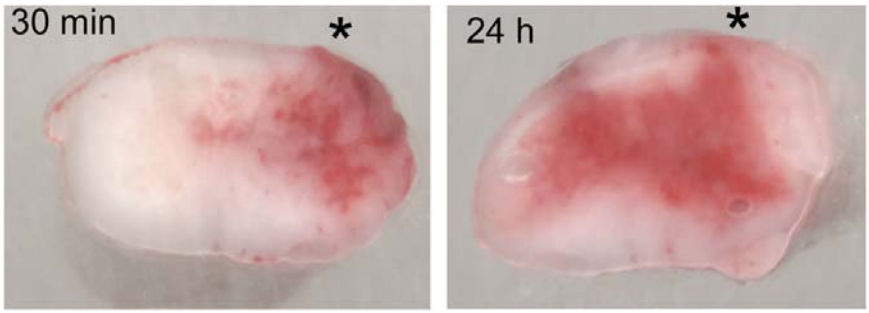

Fig. S3. Cervical hemicord contusion incites progressive hemorrhagic necrosis with minimal primary white matter damage. Cross sections of rat spinal cords harvested 30 min and 24 h after a cervical hemi-cord injury produced as described, with the impact site marked by an asterisk; the rats were perfused to remove intravascular blood. These images show: (i) grossly intact spinal cords with intact pia and no mechanical disruption of tissues; (ii) primary hemorrhage at 30 min that is confined mostly to ipsilateral grey matter; (iii) primary plus secondary hemorrhage at 24 h, after the hemorrhage has expanded into contralateral grey and white matter. Unlike some models of SCI in which bilateral primary hemorrhage may mask the benefit of halting PHN, the hemicord contusion model described is associated with modest primary injury to white matter and robust PHN, with much of the eventual tissue damage and neurological dysfunction being due to PHN and downstream secondary injury mechanisms (*6, 7*).

Supplemental References

1. J. C. Fleming, M. D. Norenberg, D. A. Ramsay, G. A. Dekaban, A. E. Marcillo, A. D. Saenz, M. Pasquale-Styles, W. D. Dietrich, L. C. Weaver, The cellular inflammatory response in human spinal cords after injury. *Brain* **129**, 3249-3269 (2006).
2. V. Gerzanich, A. Ivanov, S. Ivanova, J. B. Yang, H. Zhou, Y. Dong, J. M. Simard, Alternative splicing of cGMP-dependent protein kinase I in angiotensin-hypertension: novel mechanism for nitrate tolerance in vascular smooth muscle. *Circ. Res.* **93**, 805-812 (2003).
3. F. F. Yan, C. W. Lin, E. A. Cartier, S. L. Shyng, Role of ubiquitin-proteasome degradation pathway in biogenesis efficiency of {beta}-cell ATP-sensitive potassium channels. *Am. J. Physiol Cell Physiol* **289**, C1351-C1359 (2005).
4. J. S. Soblosky, J. H. Song, D. H. Dinh, Graded unilateral cervical spinal cord injury in the rat: evaluation of forelimb recovery and histological effects. *Behav. Brain Res.* **119**, 1-13 (2001).
5. J. C. Gensel, C. A. Tovar, F. P. Hamers, R. J. Deibert, M. S. Beattie, J. C. Bresnahan, Behavioral and histological characterization of unilateral cervical spinal cord contusion injury in rats. *J. Neurotrauma* **23**, 36-54 (2006).
6. J. M. Simard, O. Tsymbalyuk, A. Ivanov, S. Ivanova, S. Bhatta, Z. Geng, S. K. Woo, V. Gerzanich, Endothelial sulfonylurea receptor 1-regulated NC(Ca-ATP) channels mediate progressive hemorrhagic necrosis following spinal cord injury. *J. Clin. Invest* **117**, 2105-2113 (2007).

7. V. Gerzanich, S. K. Woo, R. Vennekens, O. Tsymbalyuk, S. Ivanova, A. Ivanov, Z. Geng, Z. Chen, B. Nilius, V. Flockerzi, M. Freichel, J. M. Simard, De novo expression of Trpm4 initiates secondary hemorrhage in spinal cord injury. *Nat. Med.* **15**, 185-191 (2009).